# Magnetic Properties of the Spin Tetramer Compound $Ba_6La_2Fe_4O_{15}$

Kyosuke Abe,* Yoshihiro Doi, and Yukio Hinatsu

*Division of Chemistry, Graduate School of Science, Hokkaido University, Sapporo 060-0810, Japan*

Kenji Ohoyama

*Institute for Materials Research, Tohoku University, Sendai 980-8577, Japan*

*Received July 16, 2005. Revised Manuscript Received October 21, 2005*

The crystal structure and magnetic properties for quaternary oxide $Ba_6La_2Fe_4O_{15}$ have been investigated. This compound has a hexagonal structure in which four Fe ions per formula unit occupy the sites in one $FeO_6$ octahedron and three $FeO_4$ tetrahedra. These polyhedra form a larger unit $Fe_4O_{15}$ cluster by corner sharing. This cluster shows behavior characteristic of a magnetic tetramer with a ferrimagnetic ground state of the total spin $S_T = 5$ by the antiferromagnetic interaction between $Fe^{3+}$ ions. From the magnetic susceptibility and specific heat measurements, we observed an antiferromagnetic transition at 12.8 K. The magnetic structure was determined by power neutron diffraction at 2.3 K, which indicates that the transition is due to the long-range antiferromagnetic ordering of the $Fe_4O_{15}$ clusters. The ordered magnetic moment for each $Fe^{3+}$ ion is determined to be $\sim 4\ \mu_B$. In addition, it is found that the antiferromagnetic structure changes to a ferromagnetic structure of clusters in an applied field of $\sim 2$ T (at 1.8 K).

## Introduction

Magnetically frustrated materials have been of great interest because of their unusual magnetic properties.[1,2] Most of these systems have a lattice based on a triangular or tetrahedral array of magnetic ions: triangular, kagomé, pyrochlore, and fcc lattices. When the magnetic ions adopt such a lattice and there exists an antiferromagnetic interaction between the nearest-neighbor magnetic ions, the ions can show magnetic frustration. For instance, pyrochlore oxides have been vigorously investigated; some of them show a spin−ice state.[3,4] To explore new interesting materials, researchers are now looking into compounds with more complicated lattices.[5,6]

Here, we focus our attention on the magnetic properties of quaternary oxide $Ba_6La_2Fe_4O_{15}$. This compound was first synthesized by Mevs and Müller-Buschbaum.[7] Its crystal structure is shown in Figure 1a. This compound has a hexagonal structure with space group $P6_3mc$; the $Fe^{3+}$ ions occupy two kinds of crystallographic sites (2*b* and 6*c*) and form an $FeO_6$ octahedron and three $FeO_4$ tetrahedra per formula unit, respectively. These four polyhedra are connected by corner sharing and can be regarded as an $Fe_4O_{15}$ cluster in which Fe ions arrange in the tetrahedral manner (Figure 1b). Thus, this compound may show an anomalous magnetic behavior reflecting such a structural feature. The magnetic susceptibility of this compound was previously measured;[8] however, the data, except for the information on the Néel temperature (14 K), to the best of our knowledge, have not been reported until now.

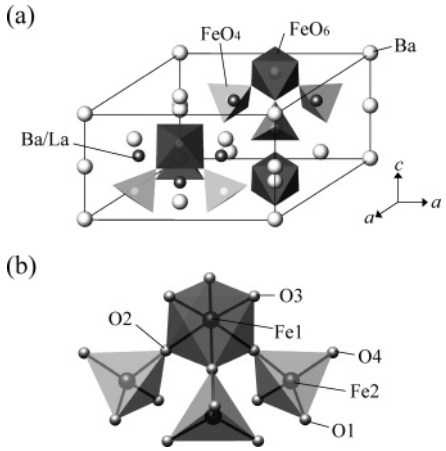


**Figure 1.** Crystal structures of (a) $Ba_6La_2Fe_4O_{15}$ and (b) the $Fe_4O_{15}$ cluster.

In this paper, we report the crystal structure and detailed magnetic properties of $Ba_6La_2Fe_4O_{15}$. To elucidate its magnetic behavior, we have performed magnetic susceptibility, specific heat, and neutron diffraction measurements. The specific heat for nonmagnetic $Ba_6La_2Ga_4O_{15}$ has also been measured to estimate the magnetic entropy change due to the magnetic ordering of Fe ions in $Ba_6La_2Fe_4O_{15}$.

* To whom correspondence should be addressed. E-mail: k-abe@sci.hokudai.ac.jp.

(1) Greedan, J. E. *J. Mater. Chem.* **2001**, *11*, 37−53.
(2) Ramirez, A. P. *Annu. Rev. Mater. Sci.* **1994**, *24*, 453−480.
(3) Ramirez, A. P.; Hayashi, A.; Cava, R. J.; Siddharthan, R.; Shastry, B. S. *Nature* **1999**, *399*, 333−335.
(4) Matsuhira, K.; Hinatsu, Y.; Tenya, K.; Sakakibara, T. *J. Phys.: Condens. Matter* **2000**, *12*, L649−L656.
(5) Rogado, N.; Lawes, G.; Huse, D. A.; Ramirez, A. P.; Cave, R. J. *Solid State Commun.* **2002**, *124*, 229−233.
(6) Lawes, G.; Kenzelmann, M.; Rogado, N.; Kim, K. H.; Jorge, G. A.; Cava, R. J.; Aharony, A.; Entin-Wohlman, O.; Harris, A. B.; Yildirim, T.; Huang, Q. Z.; Park, S.; Broholm, C.; Ramirez, A. P. *Phys. Rev. Lett.* **2004**, *93*, 247201.
(7) Mevs, H.; Muller-Büschbaum, H. *J. Less-Common Met.* **1990**, *157*, 173−178.
(8) Kudryavtsev, D. A.; Mill', B. V.; Vedernikov, N. F.; Shaplygin, I. S. *Inorg. Mater.* **1992**, *28*, 943−946.

10.1021/cm0515552 CCC: $33.50 
Published on Web 01/11/2006

## Experimental Section

$Ba_6La_2Fe_4O_{15}$ was prepared by solid-state reaction in air. For starting materials, we used $La_2O_3$, $BaCO_3$, and $Fe_2O_3$. Before use, $La_2O_3$ was dried at 1173 K overnight. Stoichiometric amounts of the compounds were mixed in an agate mortar. The mixtures were pressed into pellets and then fired in air at 1173 K for 12 h and 1573 K for 24 h with intermediate grindings and pelletings. In addition, we prepared isostructural compound $Ba_6La_2Ga_4O_{15}$ by heating stoichiometric mixtures of $La_2O_3$, $BaCO_3$, and $Ga_2O_3$ in air at 1373 K for 12 h.

The X-ray diffraction measurements were taken at room temperature in the range $10° \le 2\theta \le 120°$ using a $2\theta$ step size of 0.02° with Cu Kα radiation on a Rigaku MultiFlex diffractometer. Powder neutron diffraction measurements were carried out at 2.3 and 20 K in the range $3° \le 2\theta \le 153°$ at intervals of 0.1° with a 1.82035 Å wavelength, using the Kinken powder diffractometer for high-efficiency and high-resolution measurement, HERMES, at the Institute for Materials Research (IMR), Tohoku University,[9] installed at the JRR-3M Reactor in the Japan Atomic Energy Agency (JAEA), Tokai. The X-ray and neutron diffraction data were analyzed by the Rietveld technique, using the program RIETAN2000.[10] A small amount (<2.3%) of the $LaFeO_3$ impurity phase[11,12] was detected in both diffraction patterns; its diffraction peaks (both nuclear and magnetic reflections) were also fitted as a second phase.

The temperature dependence of the magnetic susceptibilities was measured under both zero-field-cooled (ZFC) and field-cooled (FC) conditions in an applied field of 0.1 T over the temperature range 1.8−400 K using the SQUID magnetometer (Quantum Design, MPMS-5S). The field dependence of magnetization was measured at 1.8, 10, 15, 20, and 30 K by changing the applied magnetic field between 0 and 5 T.

Specific heat measurements were performed using a relaxation technique with a commercial physical property measurement system (Quantum Design, PPMS model) in the temperature range 1.8−300 K. The sintered sample in the form of a pellet was mounted on a thin alumina plate with grease for better thermal contact.

## Results and Discussion

**Crystal Structure.** The powder neutron diffraction profile at 20 K is plotted in Figure 2a. The X-ray and neutron diffraction data for $Ba_6La_2Fe_4O_{15}$ were indexed with a hexagonal unit cell, space group $P6_3mc$. These diffraction data were analyzed by the Rietveld method using a structural model reported previously.[7] The refined lattice parameters are $a = 11.8816(4)$ Å and $c = 7.0714(2)$ Å, which are in good agreement with previous results. The structural parameters at 20 K are listed in Table 1, and the crystal structure of $Ba_6La_2Fe_4O_{15}$ is illustrated in Figure 1a.

In this structure, the Fe ions occupy two kinds of crystallographic sites (Fe1, 2*b;* and Fe2, 6*c*) and are coordinated by the six and four oxygen ions, respectively. One $FeO_6$ octahedron and three $FeO_4$ tetrahedra are linked by sharing corner oxygen ions (O2), and thus they form an $Fe_4O_{15}$ cluster (see Figure 1b). Some bond lengths and angles determined by the neutron diffraction measurements are summarized in Table 2. The interatomic distances between Fe1 and O are 2.123(6) Å for Fe1−O2 and 1.964(5) Å for Fe1−O3, and those between Fe2 and O are 1.964(6) Å for Fe2−O2, 1.855(4) Å for Fe2−O1, and 1.813(5) Å for Fe2−O4. These results indicate that the $Fe1O_6$ octahedron and $Fe2O_4$ tetrahedron are somewhat distorted in shape.

We also synthesized nonmagnetic compound $Ba_6La_2Ga_4O_{15}$ to estimate the lattice specific heat of $Ba_6La_2Fe_4O_{15}$. Its crystal structure was determined by powder X-ray diffraction measurements. It is found that this compound

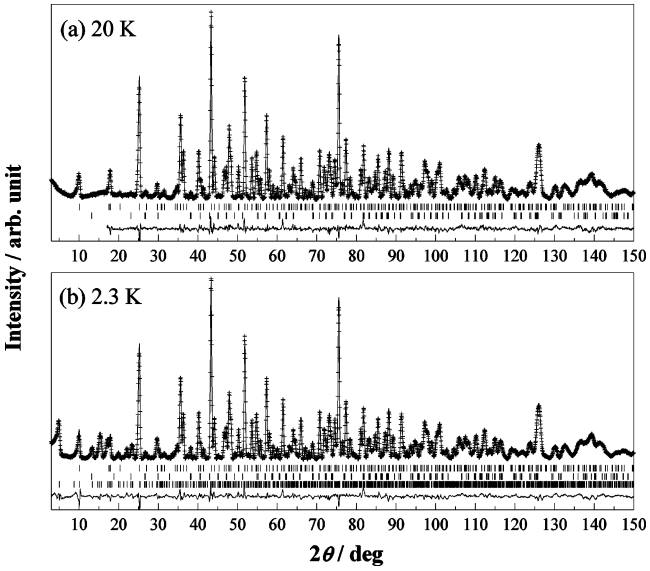


**Figure 2.** Powder neutron diffraction profiles for $Ba_6La_2Fe_4O_{15}$ at (a) 20 K and (b) 1.8 K. The upper and lower vertical marks in (a) represent the peak positions for the nuclear reflection of $Ba_6La_2Fe_4O_{15}$ and impurity $LaFeO_3$ (both magnetic and nuclear reflections), respectively. In (b), those for magnetic reflections of $Ba_6La_2Fe_4O_{15}$ are added as vertical marks at the bottom.

**Table 1. Structural Parameters for $Ba_6La_2Fe_4O_{15}$ Determined by the Neutron Diffraction Measurements at 20 and 2.3 K**

| atom | site | occupancy | *x* | *y* | *z* | *B* (Å$^2$) |
|---|---|---|---|---|---|---|
| | | | $T = 20$ K[a] | | | |
| Ba1 | 2*a* | 1.0 | 0 | 0 | 0 | 0.16(5) |
| Ba2 | 6*c* | 1.0 | 0.1736(2) | 0.8267 | 0.1607(7) | 0.16 |
| Ba3 | 2*b* | 1.0 | 1/3 | 2/3 | 0.4720(8) | 0.16 |
| Ba4 | 6*c* | 0.33333 | 0.4780(1) | 0.5220 | 0.8247(4) | 0.16 |
| La | 6*c* | 0.66667 | 0.4780 | 0.5220 | 0.8247 | 0.16 |
| Fe1 | 2*b* | 1.0 | 1/3 | 2/3 | 0.0166(7) | 0.40(5) |
| Fe2 | 6*c* | 1.0 | 0.1770(1) | 0.8230 | 0.6576(4) | 0.40 |
| O1 | 12*d* | 1.0 | 0.6749(3) | 0.0661(2) | 0.0216(5) | 0.99(5) |
| O2 | 6*c* | 1.0 | 0.2497(2) | 0.7503 | 0.8351(7) | 0.99 |
| O3 | 6*c* | 1.0 | 0.4140(2) | 0.5860 | 0.1630(7) | 0.99 |
| O4 | 6*c* | 1.0 | 0.9034(2) | 0.0966 | 0.2669(6) | 0.99 |
| | | | $T = 2.3$ K[b] | | | |
| Ba1 | 2*a* | 1.0 | 0 | 0 | 0 | 0.14(3) |
| Ba2 | 6*c* | 1.0 | 0.1737(2) | 0.8263 | 0.1626(8) | 0.14 |
| Ba3 | 2*b* | 1.0 | 1/3 | 2/3 | 0.4759(9) | 0.14 |
| Ba4 | 6*c* | 0.33333 | 0.4780(1) | 0.5220 | 0.8259(4) | 0.14 |
| La | 6*c* | 0.66667 | 0.4780 | 0.5220 | 0.8259 | 0.14 |
| Fe1 | 2*b* | 1.0 | 1/3 | 2/3 | 0.0196(6) | 0.35(3) |
| Fe2 | 6*c* | 1.0 | 0.1768(1) | 0.8232 | 0.6586(4) | 0.35 |
| O1 | 12*d* | 1.0 | 0.6751(3) | 0.0657(2) | 0.0241(5) | 0.88(2) |
| O2 | 6*c* | 1.0 | 0.2497(2) | 0.7503 | 0.8362(6) | 0.88 |
| O3 | 6*c* | 1.0 | 0.4139(2) | 0.5861 | 0.1640(7) | 0.88 |
| O4 | 6*c* | 1.0 | 0.9041(2) | 0.0959 | 0.2662(6) | 0.88 |

[a] Space group $P6_3mc$. $a = 11.8816(4)$ Å, $c = 7.0714(2)$ Å, $R_{wp} = 6.18\%$, $R_e = 3.24\%$, $R_I = 1.78\%$. [b] Space group $P6_3mc$. $a = 11.8816(2)$ Å, $c = 7.0713(1)$ Å, $R_{wp} = 6.32\%$, $R_e = 2.07\%$, $R_I$ (crystal) = 1.68%, $R_I$ (magnetic) = 1.75%. $\mu_{Fe1} = 3.82(7)\ \mu_B$, $\mu_{Fe2} = 4.10(5)\ \mu_B$.

(9) Ohoyama, K.; Kanouchi, T.; Nemoto, K.; Ohashi, M.; Kajitani, T.; Yamaguchi, Y. *Jpn. J. Appl. Phys.* **1998**, *37*, 3319−3326.
(10) Izumi, F.; Ikeda, T. *Mater. Sci. Forum* **2000**, *321−324*, 198−203.
(11) Geller, S.; Wood, E. A. *Acta Crystallogr.* **1965**, *9*, 563−568.
(12) Koehler, W. C.; Wollan, E. O. *J. Phys. Chem. Solids* **1957**, *2*, 100−106.

**Table 2. Bond Lengths and Angles for the $Fe_4O_{15}$ Cluster**

| | | | |
|---|---|---|---|
| Bond Length (Å) | | | |
| Fe1−O3 (×3) | 1.964(5) | Fe2−O4 (×1) | 1.813(5) |
| Fe1−O2 (×3) | 2.123(6) | Fe2−O1 (×2) | 1.855(4) |
| | | Fe2−O2 (×1) | 1.964(6) |
| Bond Angles (deg) | | | |
| Fe1−O2−Fe2 | 176.8(3) | O1−Fe2−O1 | 112.1(2) |
| O2−Fe1−O2 | 87.9(2) | O1−Fe2−O4 | 114.0(1) |
| O2−Fe1−O3 | 88.6(1) | O2−Fe2−O4 | 115.0(2) |
| O3−Fe1−O3 | 94.6(2) | O1−Fe2−O2 | 100.1(1) |

**Table 3. Structural Parameters for $Ba_6La_2Ga_4O_{15}$[a] Determined by the X-ray Diffraction Measurement**

| atom | site | occupancy | *x* | *y* | *z* | *B* (Å$^2$) |
|---|---|---|---|---|---|---|
| Ba1 | 2*a* | 1.0 | 0 | 0 | 0 | 0.87(3) |
| Ba2 | 6*c* | 1.0 | 0.1724(1) | 0.8276 | 0.1703(7) | 0.87 |
| Ba3 | 2*b* | 1.0 | 1/3 | 2/3 | 0.4873(7) | 0.87 |
| Ba4 | 6*c* | 0.33333 | 0.4789(1) | 0.5211 | 0.8377(5) | 0.87 |
| La | 6*c* | 0.66667 | 0.4789 | 0.5211 | 0.8377 | 0.87 |
| Ga1 | 2*b* | 1.0 | 1/3 | 2/3 | 0.0440(9) | 0.81(5) |
| Ga2 | 6*c* | 1.0 | 0.1784(2) | 0.8216 | 0.6780(7) | 0.81 |
| O1 | 12*d* | 1.0 | 0.685(1) | 0.068(1) | 0.052(1) | 1.0(2) |
| O2 | 6*c* | 1.0 | 0.252(1) | 0.748 | 0.863(3) | 1.0 |
| O3 | 6*c* | 1.0 | 0.415(1) | 0.585 | 0.178(3) | 1.0 |
| O4 | 6*c* | 1.0 | 0.905(1) | 0.095 | 0.276(2) | 1.0 |

[a] At room temperature. Space group $P6_3mc$. $a$ = 11.8426(6) Å, $c$ = 7.0900(3) Å, $R_{wp}$ = 9.37%, $R_e$ = 6.71%, $R_I$ = 2.90%.

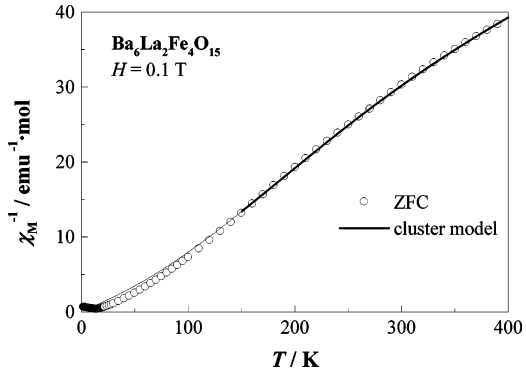


**Figure 3.** Temperature dependence of the inverse magnetic susceptibility for $Ba_6La_2Fe_4O_{15}$. The solid line represents a fitting curve using the magnetic cluster model (see text).

adopts the same structure as $Ba_6La_2Fe_4O_{15}$. Table 3 shows structural parameters for this compound.

**Magnetic Susceptibility at Higher Temperatures.** The temperature dependence of the inverse magnetic susceptibility for $Ba_6La_2Fe_4O_{15}$ is plotted in Figure 3. It shows a poor linearity in the high-temperature region and does not obey the Curie−Weiss law. The effective magnetic moment, estimated from the magnetic susceptibility at room temperature, was $\mu_{eff}$ = 8.96 $\mu_B$. This value is much smaller than the value of 11.83 $\mu_B$ calculated from the free-ion ($S$ = 5/2) magnetic moment per formula unit. It is believed that these experimental results reflect the structural characteristics of this compound, i.e., Fe ions form the $Fe_4O_{15}$ cluster. If the magnetic interaction between Fe ions in this cluster is much stronger than that between clusters, it may be possible that the cluster is magnetically isolated. In this case, the exchange Hamiltonian is written as follows

$$H_{ex} = -2J_1(S_1S_2 + S_1S_3 + S_1S_4) - 2J_2(S_2S_3 + S_2S_4 + S_3S_4) \quad (1)$$

where $J_1$ and $J_2$ denote the exchange integrals between Fe1−Fe2 and Fe2−Fe2, respectively; $S_1$ is the spin for Fe1; and $S_2$, $S_3$, and $S_4$ are spins for Fe2 (see Figure 1b). The eigenvalues are given by the following

$$E(S_T,S') = -J_1S_T(S_T + 1) + (J_1 - J_2)S'(S' + 1) + \text{constant} \quad (2)$$

where $S_T$ and $S'$ mean the spin quantum numbers for $S_T = S_1 + S_2 + S_3 + S_4$ and $S' = S_2 + S_3 + S_4$. Thus, the molar magnetic susceptibility is given by the Van-Vleck equation

$$\chi_{cluster} = \frac{N_A g^2 \mu_B{}^2}{3k_BT} \frac{\sum_{S_T,S'} S_T(S_T + 1)(2S_T + 1)e^{-E(S_T,S')/k_BT}}{\sum_{S_T,S'} (2S_T + 1)e^{-E(S_T,S')/k_BT}} \quad (3)$$

The magnetic susceptibility calculated by this model ($T$ > 200 K) is shown as a solid line in Figure 3 and is in good agreement with the experimental data. The exchange integrals are determined to be $J_1$ = −35.1(1) K and $J_2$ = −3.41(2) K. This result shows the existence of two kinds of antiferromagnetic interactions, one between Fe1 and Fe2 and the other between Fe2 and Fe2 ions. $|J_1|$ is about 10 times larger than $|J_2|$, which reflects the difference in the interaction pathway between Fe ions, i.e., the linear superexchange pathway (Fe1−O−Fe2) and the much weaker super-superexchange pathway (Fe2−O−O−Fe2). Thus, the magnetic ground state of the $Fe_4O_{15}$ cluster becomes a ferrimagnetic arrangement ($S_T$ = 5 and $S'$ = 15/2).

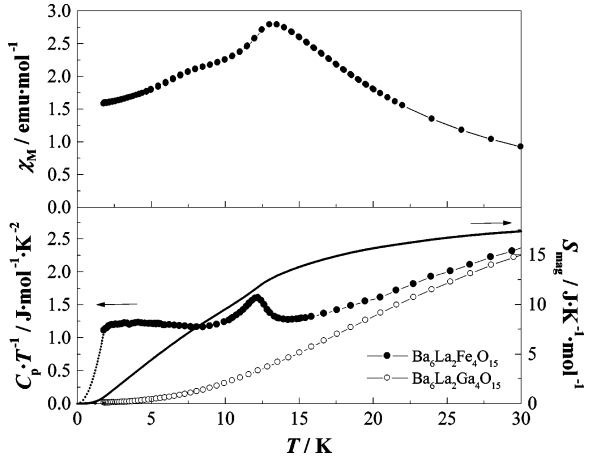


**Figure 4.** Temperature dependences of (a) magnetic susceptibility ($\chi_M$) and (b) specific heat divided by temperature ($C_p/T$) and magnetic entropy ($S_{mag}$) for $Ba_6La_2Fe_4O_{15}$. The specific heat divided by temperature for the nonmagnetic $Ba_6La_2Ga_4O_{15}$ is also plotted. The data below 1.8 K were extrapolated by $C_p \propto T^3$ (dotted curves).

**Magnetic Transition at Low Temperature.** The temperature dependence of the magnetic susceptibility (below 30 K) is plotted in Figure 4 a. The ZFC and FC susceptibilities are almost the same throughout the whole temperature range. It is found that this compound shows an antiferromagnetic transition at 12.8 K, which is in good agreement with previous reports.[8] The temperature dependence of the specific heat is shown in Figure 4b. A specific heat anomaly is observed at the same temperature. These results indicate that a long-range antiferromagnetic ordering of $Fe^{3+}$ ions occurs at this temperature.

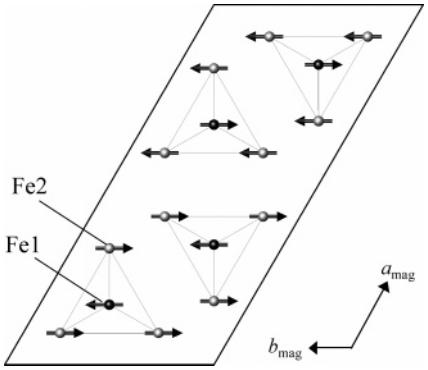


**Figure 5.** Magnetic structure of $Ba_6La_2Fe_4O_{15}$. The arrows represent the direction of the magnetic moment for $Fe^{3+}$ ions.

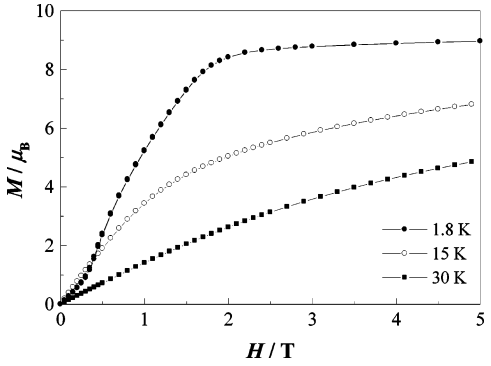


**Figure 6.** Magnetization as a function of the applied magnetic field for $Ba_6La_2Fe_4O_{15}$ at several temperatures.

To estimate the magnetic entropy change ($\Delta S_{mag}$) associated with this magnetic transition, we estimated the magnetic specific heat ($C_{mag}$) by subtracting the lattice specific heat from the experimental specific heat of $Ba_6La_2Fe_4O_{15}$. For the lattice contribution, we used the specific heat of the nonmagnetic compound $Ba_6La_2Ga_4O_{15}$. The temperature dependence of the magnetic entropy is shown in Figure 4b. The magnetic entropy change is about 17.4 J $mol^{-1}$ $K^{-1}$ at 30 K.

If this transition is due to the ordering of fully paramagnetic $Fe^{3+}$ ($S = 5/2$) ions, the magnetic entropy change is expected to be $4R \ln(2S + 1) = 59.6$ J $mol^{-1}$ $K^{-1}$. The observed entropy change is obviously smaller than this value. This discrepancy arises from the fact that the $Fe^{3+}$ ions are not fully paramagnetic but form the magnetic cluster. From the values of $J_1$ and $J_2$, the ground and first excited states of this cluster are $S_T = 5$, $S'' = 15/2$ and $S_T = 4$, $S'' = 13/2$, respectively, and the energy difference between them is 124.6 K. Thus, the ground state is selectively populated (97.5%) at 30 K. The multiplicity of this state is 11, and the expected entropy change is $R \ln 11 = 19.9$ J $mol^{-1}$ $K^{-1}$. This value is in good agreement with the experimental one (17.4 J $mol^{-1}$ $K^{-1}$). Therefore, we conclude that the observed magnetic transition is due to the magnetic ordering of $Fe_4O_{15}$ clusters with $S_T = 5$.

**Magnetic Structure.** The powder neutron diffraction profile for $Ba_6La_2Fe_4O_{15}$ at 2.3 K is shown in Figure 2b. In this profile, some additional reflection peaks were found at lower angles that were not observed at 20 K. They are associated with the long-range ordering of $Fe^{3+}$ magnetic moments. These peaks can be indexed using a propagation vector $\mathbf{k} = (1/2, 0, 0)$, i.e., the magnetic unit cell is represented as $a_{mag} = 2a$, $b_{mag} = b$, and $c_{mag} = c$.

To determine the magnetic structure, we assumed that the magnetic moment of the Fe1 ion was antiparallel to three Fe2 magnetic moments in an $Fe_4O_{15}$ cluster (because it has a large negative $J_1$) and that all the Fe moments are collinear. The determined magnetic structure is illustrated in Figure 5, and the refined structural parameters are listed in Table 1. In this magnetic structure, the ferrimagnetic moment in the $Fe_4O_{15}$ cluster orders antiferromagnetically, and the direction of the magnetic moments is parallel or antiparallel to the *b*-axis. The ordered magnetic moments of the Fe ions are 3.82(7) $\mu_B$ for Fe1 and 4.10(5) $\mu_B$ for Fe2. These values

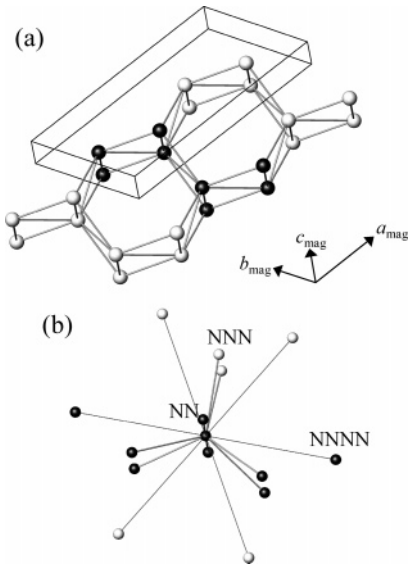


**Figure 7.** Schematic illustration for the arrangement of $Fe_4O_{15}$ clusters: (a) honeycomb-like framework and (b) coordination geometry. The circles represent the position of the clusters (atomic position of Fe1 ion); the filled and open symbols represent the direction opposite that of the magnetic moment of the cluster.

are smaller than the value of 5 $\mu_B$ expected for the $Fe^{3+}$ ion, which is relevant to the fact that the magnetic specific heat below $T_N$ does not readily drop with decreasing temperature (see Figure 4). These results may be due to the existence of the magnetic frustration between Fe ions by the tetrahedral array.

**Magnetization Measurement.** The magnetization as a function of the applied magnetic field at different temperatures is shown in Figure 6. All the data show no hysteresis loop; however, saturation of the magnetization ($\sim$8.9 $\mu_B$) is observed for the 1.8 K data. This moment is about half of the full magnetization of this system (20 $\mu_B$); the observed saturation-like behavior is actually an intermediate plateau. This result indicates the occurrence of the spin−flip transition of the $Fe_4O_{15}$ clusters, i.e., a change in magnetic structure from antiferromagnetic to ferromagnetic ordering, keeping the nature of the cluster ground state with $S_T = 5$.

**Magnetic Interaction between Clusters.** In this structure, each cluster is surrounded by two nearest-neighbor clusters (NN; the distance is 7.07 Å), six next-nearest-neighbor clusters (NNN; 7.72 Å), and six next-next-nearest-neighbor clusters (NNNN; 11.88 Å). The schematic illustration is shown in Figure 7. They form a triangle-based lattice that resembles

a honeycomb. The determined magnetic structure is, on the whole, antiferromagnetic; however, it is actually a combination of the antiferromagnetic and ferromagnetic arrangements.

The coupling to the NN clusters is completely ferromagnetic. The temperature dependence of the experimental magnetic susceptibility below ~150 K shows the positive deviation from the calculated susceptibility on the basis of the cluster model, which indicates that ferromagnetic interaction with the NN clusters is predominant around this temperature region.

On the other hand, magnetic couplings to the NNN and NNNN clusters occur with antiferromagnetic:ferromagnetic ratios of 2:4 and 4:2, respectively. There exists a competition between the ferromagnetic (NNN) and antiferromagnetic (NNNN) interactions at low temperatures. The spin−flip transition observed in $H \approx 2$ T at 1.8 K indicates that the former interaction is more advantageous than the latter when a magnetic field is applied.

## Summary

The crystal structure and magnetic properties for the $Ba_6La_2Fe_4O_{15}$ containing the $Fe^{3+}$ ion have been investigated. This compound has a hexagonal structure with space group $P6_3mc$ and forms the $Fe_4O_{15}$ cluster. This cluster behaves as a magnetic tetramer with a ground state of $S_T = 5$ that is derived from the relatively strong intracluster interaction between Fe1−Fe2 ions ($J_1 = -35.1(1)$ K). At 12.8 K, this compound shows an antiferromagnetic transition, which is due to the long-range antiferromagnetic ordering of the clusters, in which the ordered magnetic moment for each $Fe^{3+}$ ion is ~4 $\mu_B$. This antiferromagnetic state is easily broken by an applied magnetic field of ~2 T at 1.8 K.

**Acknowledgment.** This research was partially supported by the Ministry of Education, Culture, Sports, Science and Technology, Japan, a Grant-in-Aid for Young Scientists (16750043), and the Scientific Research Priority Areas "Panoscopic Assembling and High Ordered Functions for Rare Earth Materials" (17042003).

CM0515552